Title	Single-neuron and genetic correlates of autistic behavior in macaque
Author(s)	Yoshida, Kyoko; Go, Yasuhiro; Kushima, Itaru; Toyoda, Atsushi; Fujiyama, Asao; Imai, Hiroo; Saito, Nobuhito; Iriki, Atsushi; Ozaki, Norio; Isoda, Masaki
Citation	Science Advances (2016), 2(9)
Issue Date	2016-09-21
URL	http://hdl.handle.net/2433/224811
Right	© 2016, The Authors. This is an open-access article distributed under the terms of the Creative Commons Attribution-NonCommercial license, which permits use, distribution, and reproduction in any medium, so long as the resultant use is not for commercial advantage and provided the original work is properly cited.
Type	Journal Article
Textversion	publisher

PSYCHOLOGY

Single-neuron and genetic correlates of autistic behavior in macaque

10.1126/sciadv.1600558

Kyoko Yoshida,[1,2,3]* Yasuhiro Go,[4,5,6] Itaru Kushima,[7,8] Atsushi Toyoda,[9,10] Asao Fujiyama,[9,10,11] Hiroo Imai,[12] Nobuhito Saito,[2] Atsushi Iriki,[3] Norio Ozaki,[8] Masaki Isoda[3,5,6,13,14,15]

Atypical neurodevelopment in autism spectrum disorder is a mystery, defying explanation despite increasing attention. We report on a Japanese macaque that spontaneously exhibited autistic traits, namely, impaired social ability as well as restricted and repetitive behaviors, along with our single-neuron and genomic analyses. Its social ability was measured in a turn-taking task, where two monkeys monitor each other's actions for adaptive behavioral planning. In its brain, the medial frontal neurons responding to others' actions, abundant in the controls, were almost nonexistent. In its genes, whole-exome sequencing and copy number variation analyses identified rare coding variants linked to human neuropsychiatric disorders in 5-hydroxytryptamine (serotonin) receptor 2C (*HTR2C*) and adenosine triphosphate (ATP)–binding cassette subfamily A13 (*ABCA13*). This combination of systems neuroscience and cognitive genomics in macaques suggests a new, phenotype-to-genotype approach to studying mental disorders.

INTRODUCTION

Autism spectrum disorder (ASD) is characterized by persistent deficits in social communication and social interaction, as well as restricted, repetitive patterns of behavior, interests, or activities [*Diagnostic and Statistical Manual of Mental Disorders, Fifth Edition* (*DSM-5*)] (*1*). It is a set of heterogeneous neurodevelopmental conditions and is attributed to complex interactions between genetic and environmental factors. In recent years, there has been a growing interest in the pathophysiological mechanisms underlying cognitive behavioral features in ASD. Although some mouse models have been successfully developed (*2*), the evaluation of higher cognitive functions is difficult, and invasive experiments, such as single-neuron recording, on human subjects are only allowed in a special context, that is, in association with medical treatment. The monkey that we report here displayed an impaired ability to monitor others' actions, an obsession with systems, and repetitive behavior, which are most frequently associated with ASD. To understand the mechanisms underlying these signs, particularly the impaired ability to monitor others' actions, we performed a range of behavioral analyses, single-neuron recording in the medial frontal cortex (MFC)—the hub of social brain networks (*3*, *4*), and genetic typing of the monkey.

[1]Japan Community Healthcare Organization Yugawara Hospital, Yugawara, Kanagawa, Japan. [2]Department of Neurosurgery, The University of Tokyo Graduate School of Medicine, Hongo, Tokyo, Japan. [3]Laboratory for Symbolic Cognitive Development, RIKEN Brain Science Institute, Wako, Saitama, Japan. [4]Department of Brain Sciences, Center for Novel Science Initiatives, National Institutes of Natural Sciences, Okazaki, Aichi, Japan. [5]Department of System Neuroscience, National Institute for Physiological Sciences, Okazaki, Aichi, Japan. [6]Department of Physiological Sciences, School of Life Science, SOKENDAI (The Graduate University for Advanced Studies), Okazaki, Aichi, Japan. [7]Institute for Advanced Research, Nagoya University, Nagoya, Aichi, Japan. [8]Department of Psychiatry, Nagoya University Graduate School of Medicine, Nagoya, Aichi, Japan. [9]Comparative Genomics Laboratory, National Institute of Genetics, Mishima, Shizuoka, Japan. [10]Advanced Genomics Center, National Institute of Genetics, Mishima, Shizuoka, Japan. [11]Department of Genetics, School of Life Science, SOKENDAI (The Graduate University for Advanced Studies), Mishima, Shizuoka, Japan. [12]Molecular Biology Section, Primate Research Institute, Kyoto University, Inuyama, Aichi, Japan. [13]Department of Physiology, Kansai Medical University School of Medicine, Hirakata, Osaka, Japan. [14]Precursory Research for Embryonic Science and Technology, Japan Science and Technology Agency, Kawaguchi, Saitama, Japan. [15]Unit on Neural Systems and Behavior, Okinawa Institute of Science and Technology, Onna, Okinawa, Japan. *Corresponding author. Email: yakouk-tky@umin.ac.jp

RESULTS

Evaluation of behavior: The ability to monitor others' action

To evaluate the ability to monitor others' actions, we devised a task called the role-reversal task for two monkeys, as described previously (*5*) (Fig. 1A). In our task, the actor monkey had to make a choice between yellow and green buttons, whereas the observer monkey was required to sit still, with the two roles alternating every two trials (Fig. 1B). Both of them were rewarded or not rewarded, depending on the color selected by the actor. The color whose selection was followed by a reward remained the same during a block of 5 to 17 successive trials, and then the color-reward association was switched without a cue (Fig. 1B). Here, each trial was designated as a self-trial or a partner's trial according to whether the actor was oneself or one's partner. Here, three male monkeys (*Macaca fuscata*; designated as N, S, and E) performed the task in three different pairs.

As the roles alternated every two trials, the actor of the previous trial was either oneself or one's partner. When the previous and current trials were nonswitch ones and the choice in the previous trial was correct, all the monkeys chose the correct color in both cases (Fig. 2A). Then, we analyzed their performance following unrewarded trials, which were classified into two types (*5*). The first type was no reward due to a block change, because the color-reward association changed without a signal. After this type of no-reward trial, the monkeys needed to switch their choice of color. In these trials, all the monkeys performed well after both self- and partner's trials (Fig. 2B). The second type was no reward due to a choice error, after which the monkeys should not switch their choice of color from that chosen in the trial before the error. In these trials (Fig. 2C, upper panels), monkey E's performance after partner's trials was extremely poor, with the percentage of correct choice being significantly lower than 50% (19.5%; $P < 10^{-4}$, Wilcoxon signed-rank test), whereas those of the other two monkeys were significantly higher than 50% (N, 87.5%; S, 86.6%; $P < 10^{-9}$), indicating that monkey E intentionally chose the wrong color. One possible explanation for this curious behavior is that monkey E switched the color following no reward, regardless of the color selected by the partner. Monkey E seemed to have developed a unique strategy with which another's action information was not required (fig. S1; see also Supplementary Text). Indeed, gaze

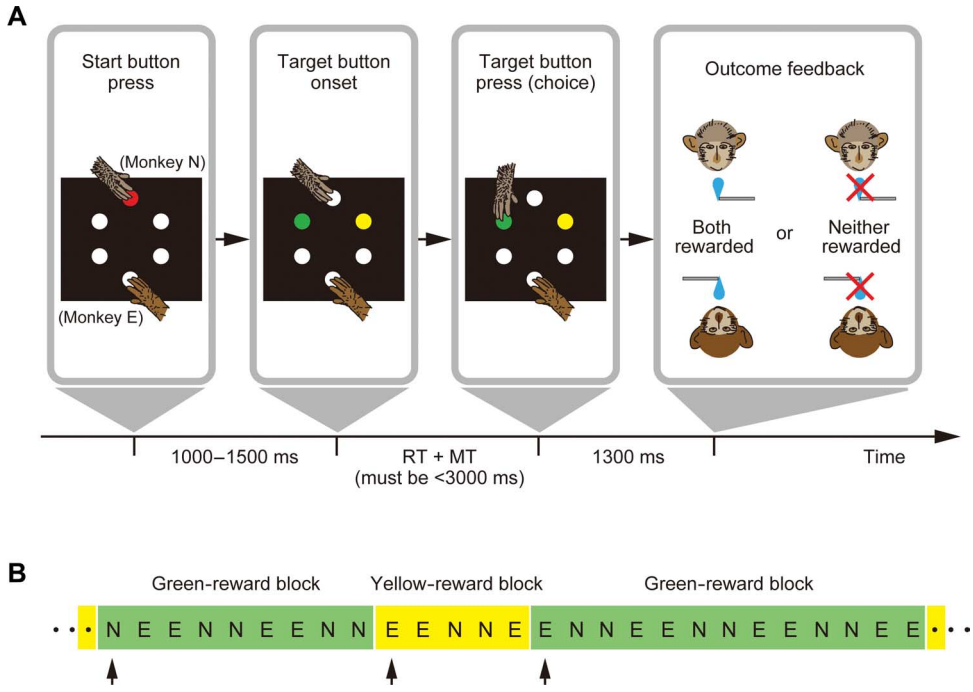

Fig. 1. Behavioral task. (**A**) Temporal sequence of events in the role-reversal task. An example of a single trial in which monkey N was the actor and monkey E was the observer is shown. After the actor had pressed a start button (illuminated in red) for 1000 to 1500 ms, two target buttons turned on in two different colors (green and yellow), the positions of which were randomized across trials. In the example shown, the actor chose the green button. Both monkeys were rewarded 1300 ms later when a reward was associated with the green target ("green-reward block"), but neither was rewarded when a reward was associated with the yellow target ("yellow-reward block"). RT, reaction time; MT, movement time. (**B**) The two different roles alternated every two trials, and the color-reward contingency was switched every 5 to 17 trials (blocked design). N and E represent the actor in each trial. Trials with and without arrows indicate SWITCH and non-SWITCH trials, respectively.

analysis revealed that monkey E did not look at the target buttons around the partner's choice while it was sitting still as the observer (fig. S2). Although this incapability to use others' action information could be regarded as a deficit, monkey E also had strong points, similar to some patients with ASD whose altered developmental emphases are considered to promote cognitive strengths (*6*). The RTs after four types of no-reward trial (choice error and error due to block change by either oneself or one's partner) in monkey E were consistent [$P = 0.76$, one-way analysis of variance (ANOVA)], whereas those in monkeys N ($P < 10^{-8}$) and S ($P < 10^{-13}$) were not (fig. S3). The constant RTs after all types of error suggest that monkey E coped with the no-reward trials in a systemized way (*6*). This systemized strategy might explain why monkey E performed better than the others after its own choice error (N, 79.7%; S, 70.9%; E, 92.7%; Fig. 2C, lower panels; see also Supplementary Text).

Monkey E's behavior was also different from that of the other monkeys outside the experimental context. First, monkey E never displayed affiliative behaviors toward the experimenters that served to initiate social interactions, such as presenting for grooming and presenting for mounting, whereas monkeys N and S showed these behaviors whenever the experimenters visited their cages (see Supplementary Text). Second, monkey E frequently showed nail-biting behavior, which is a form of stereotypy. Comparing these observations both inside and outside the task context with *DSM-5* criteria, along with the fact that the brain magnetic resonance imaging revealed no apparent structural abnormality (Fig. 3), we considered that monkey E had a particular disorder that could be called psychiatric, similar to human ASD.

Agent-related neurons in the MFC

We carried out extracellular single-unit recording in the MFC because functional changes in this area have been often observed in ASD patients (*7*). We recorded in two cortical subregions, that is, the dorsomedial convexity subregion ("MFC convexity") and the cingulate sulcus subregion ("MFC sulcus"). The MFC convexity mainly included the pre–supplementary motor area (pre-SMA; see Materials and Methods for the definition) and prefrontal area 9 (*8*) immediately rostral to the pre-SMA. The MFC sulcus was contained in the dorsal bank and fundus of the cingulate sulcus. It largely corresponded to the rostral cingulate motor area (*9*) and its rostrally adjacent prefrontal region (area 24c). In all three monkeys, we identified three types of agent-related neurons, as previously reported (*10*): "self-type neurons," which are preferentially responsive to one's own actions; "mirror-type neurons," which are equally responsive to self's and another's actions; and "partner-type neurons," which are preferentially responsive to another's actions (fig. S4). However, in monkey E, neurons responding to others' actions, that is, partner- and mirror-type neurons, were significantly less frequent ($P < 0.05$, χ^2 test), whereas self-type neurons were significantly more frequent ($P < 0.001$; Table 1) than those in the other two monkeys. Moreover, among these small numbers of partner- and mirror-type neurons, we could not find any clear example with distinct activities, in sharp contrast to the self-type neurons (Fig. 4),

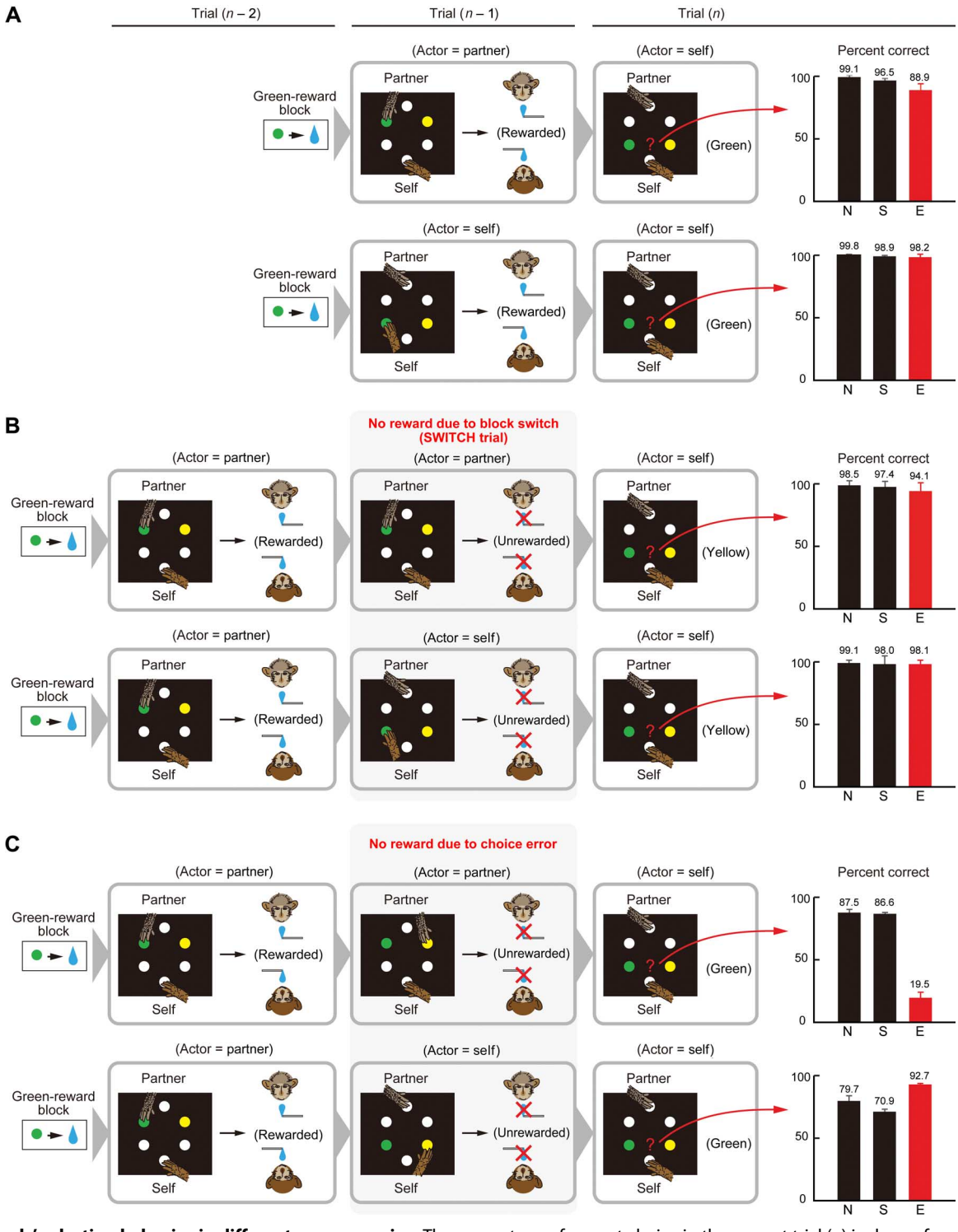

Fig. 2. Animals' selection behavior in different case scenarios. The percentage of correct choice in the current trial (*n*) is shown for each monkey in the rightmost column. Values on top of the bars represent the averages. Error bars denote SEM. In all the examples shown, the green target was initially associated with a reward (see the leftmost insets). (**A**) In the preceding trial (*n* – 1), the actor was either the partner (upper panel) or oneself (lower panel), and the actor's selection was followed by a reward. The animal to be analyzed is designated as "self." The correct target color in the trial (*n*) is indicated in parentheses. (**B**) In the preceding trial (*n* – 1), the actor was either the partner (upper panel) or oneself (lower panel), and the actor's selection was followed by no reward owing to block switches. Other conventions are the same as in (A). (**C**) In the preceding trial (*n* – 1), the actor was either the partner (upper panel) or oneself (lower panel), and the actor's selection was followed by no reward owing to a choice error. Other conventions are the same as in (A).

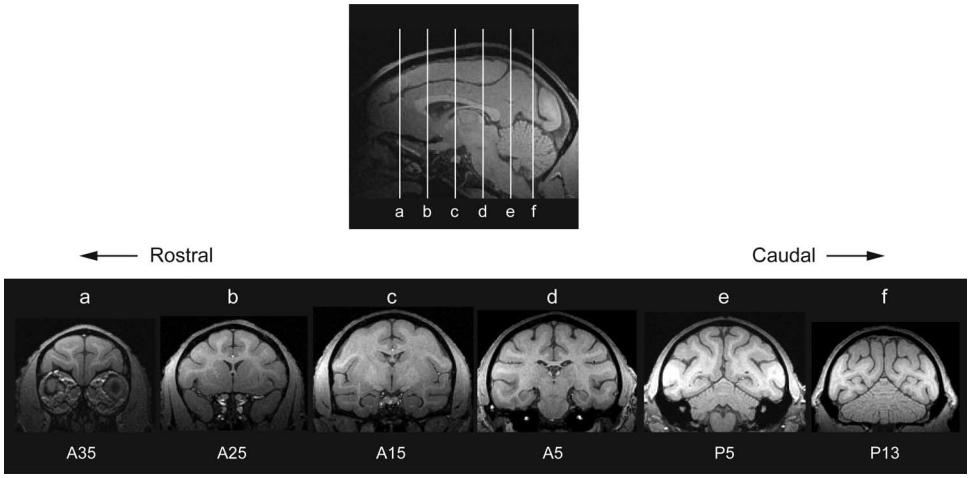

Fig. 3. T1-weighted magnetic resonance images for monkey E. Each coronal section was obtained at the rostrocaudal level indicated by a corresponding white line and lettering below. Each corresponding Horsley-Clarke stereotactic coordinate is also shown. A, anterior; P, posterior. Note that there was no gross structural abnormality.

Table 1. Number of agent-related neurons in MFC. Values denote the number of neurons. Values in parentheses denote the percentage.

	Self-type neurons	Mirror-type neurons	Partner-type neurons	Total neurons recorded
Monkey N	60 (10.0)	34 (5.7)	101 (16.8)	601
Monkey S	40 (15.3)	26 (10.0)	37 (14.2)	261
Monkey E	49 (22.8)	4 (1.9)	5 (2.3)	215

as well as those of the three types of agent-related neurons in the other two monkeys (fig. S4). This finding supports the theory that MFC neurons play an important role in social action monitoring (*10*).

Identification of rare coding genetic variants

To explore the possible genetic causes of monkey E's atypical social behavior and single-neuron populations, we performed analyses of copy number variations (CNVs) and extensive genomic sequencing (exome). We identified two different abnormalities in genes associated with human neurodevelopmental and neuropsychiatric disorders. First, by array comparative genomic hybridization (aCGH), we detected 20 CNVs (12 deletions and 8 duplications) in monkey E (table S1). Among them, a 991-kb deletion (chr3:77110419-78101380) disrupted *ABCA13* (Fig. 5, A and B), namely, adenosine triphosphate (ATP)–binding cassette subfamily A13. No other CNVs in monkey E were reported to be associated with human psychiatric disorders. The *ABCA13* deletion was validated using a high-resolution array and a real-time polymerase chain reaction (PCR)–based TaqMan copy number assay (Fig. 5C). In a control group of 335 Japanese macaques, no CNV was identified in *ABCA13*. This gene is hypothesized to code a lipid transporter (*11*) and could be a susceptibility factor not only for schizophrenia and bipolar disorder (*12*) but also for ASD (*13*, *14*) (Supplementary Text). In monkeys N and S, no CNV associated with psychiatric disorders was detected.

Second, by exome sequencing, we identified 32 genes with loss-of-function (LoF) mutations that were uniquely found in monkey E among 100 macaque monkeys, including N and S (table S2). Among them, the mutation in exon 6 of *HTR2C* [5-hydroxytryptamine (serotonin) receptor 2C] was noteworthy (Fig. 6A), because this gene has been implicated in neuropsychiatric disorders, including ASD (*2*, *15*, *16*) (Supplementary Text). No other LoF mutations in monkey E were reportedly associated with psychiatric disorders. The result of *HTR2C* mutation in monkey E was further confirmed using Sanger-based sequencing (Fig. 6B). It has been shown that *HTR2C* has two different transcripts—the full-length receptor isoform and the truncated isoform. Owing to a different codon usage in exon 6, the mutation generated a stop codon in the truncated isoform, whereas it caused no amino acid changes in the receptor isoform (Fig. 6A). Then, we quantified the expression levels of the two isoforms in various brain regions during different developmental stages in six control monkeys. Remarkably, the expression level of the truncated isoform was considerably higher in all stages (Fig. 6C) and regions (Fig. 6D), suggesting that the truncated isoform plays an important role in HTR2C signaling, at least during relatively early postnatal periods (Supplementary Text).

DISCUSSION

Here, we identified rare coding variants in *ABCA13* and *HTR2C*, reportedly linked to human neuropsychiatric disorders, in the monkey exhibiting poor ability to monitor others' actions. The monkey was quite good at monitoring and controlling its own actions. Thus, it is

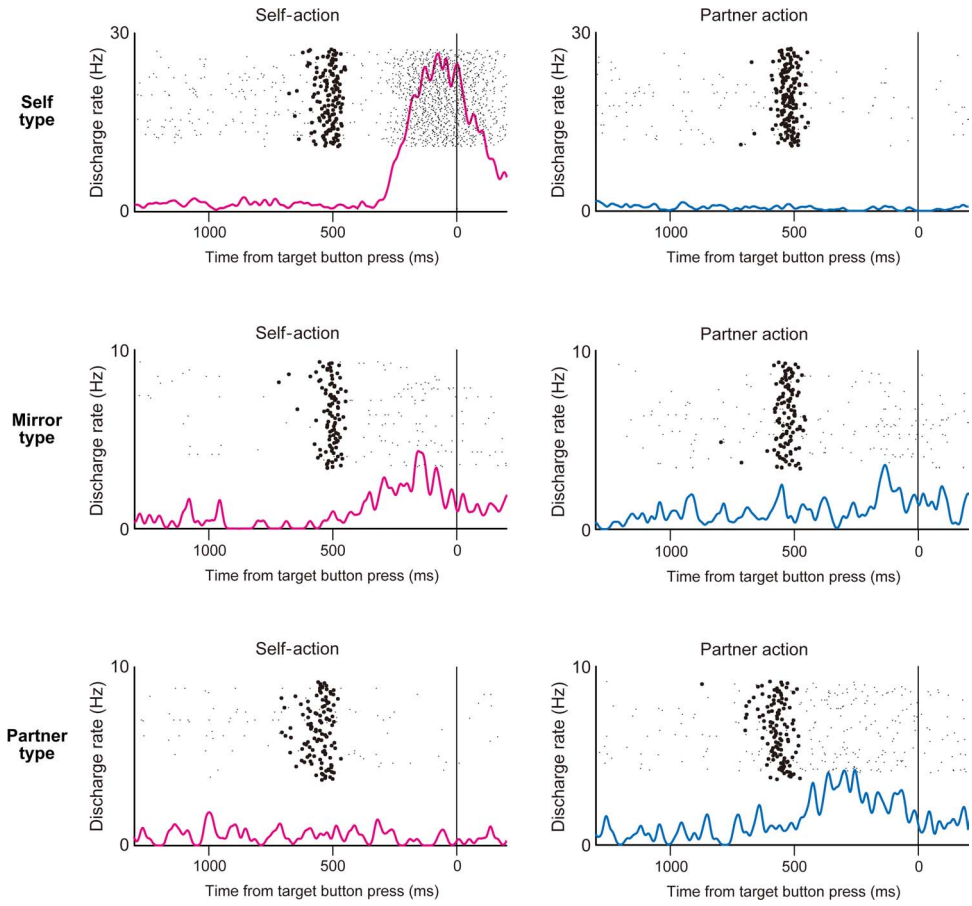

Fig. 4. Three types of agent-related neuron in the MFC of monkey E. Raster displays and spike density functions of one example each of self-type neuron (**top**), mirror-type neuron (**middle**), and partner-type neuron (**bottom**). Small black dots indicate the time of individual action potentials; large black dots indicate the time of target button onset. The displays are aligned on the time of the actor's target button pressing (vertical lines). See also fig. S4 for other examples recorded from the neurotypical monkeys.

unlikely that the behavioral disorder was due to a lack of motivation to work, problems in color discrimination, or a general impairment of performance monitoring. Instead, our findings suggest that the monkey had reduced interest in what others did or difficulties in monitoring others' actions. Atypical neuronal representation of others' actions in the MFC might be associated with impaired social action monitoring, consistent with atypical neural processing of others' actions in ASD (*17*).

In monkey E, the proportions of partner- and mirror-type neurons in the MFC were significantly smaller than those in the other monkeys. It is possible to consider that this difference in neuronal populations was due to the impaired functional integrity occurring locally within the MFC, which led to deficits in attending to and monitoring others' actions. It is also conceivable that the paucity of MFC neurons responsive to others' actions was primarily due to aberrant processing of others' actions in other brain regions that send outputs to the MFC. One of the candidates for these regions is the superior temporal sulcus (STS) of the cerebral cortex.

The STS directly projects to the MFC (*18*) and is associated with the processing of socially relevant information that culminates in the analysis of the dispositions and intentions of other individuals (*19*). This area is involved in the perception of gaze direction and mouth movements (*20*); in processing the movements of the face, arms, or whole body of others (*21*, *22*); and in processing the intentionality of observed movements (*23*). These findings suggest that relatively early processing of socially relevant information occurs in the STS. The others-related information processed in the STS may be sent to and then be integrated in the MFC to organize one's own behavior in a socially adaptive manner (*5*).

Anatomical and functional abnormalities in the STS have been highly implicated in ASD (*24*, *25*). In children with ASD, the gray-matter thickness was significantly smaller (*26*), and hypoperfusion was observed (*27*, *28*) in the bilateral STS and adjacent regions. The more severe the autistic symptoms, the lower the STS blood flow (*29*). When viewing animations of two triangles that can elicit mentalizing, an ASD population shows less activation, compared with a neurotypical population, in a mentalizing network including the STS, which mirrors less accurate descriptions of the animations (*30*). These findings raise the possibility that atypical MFC representation of others' actions in monkey E was associated with atypical neuronal processing of biological motion in the STS.

Our finding that the numbers of partner- and mirror-type MFC neurons were significantly smaller in the monkey with some autistic

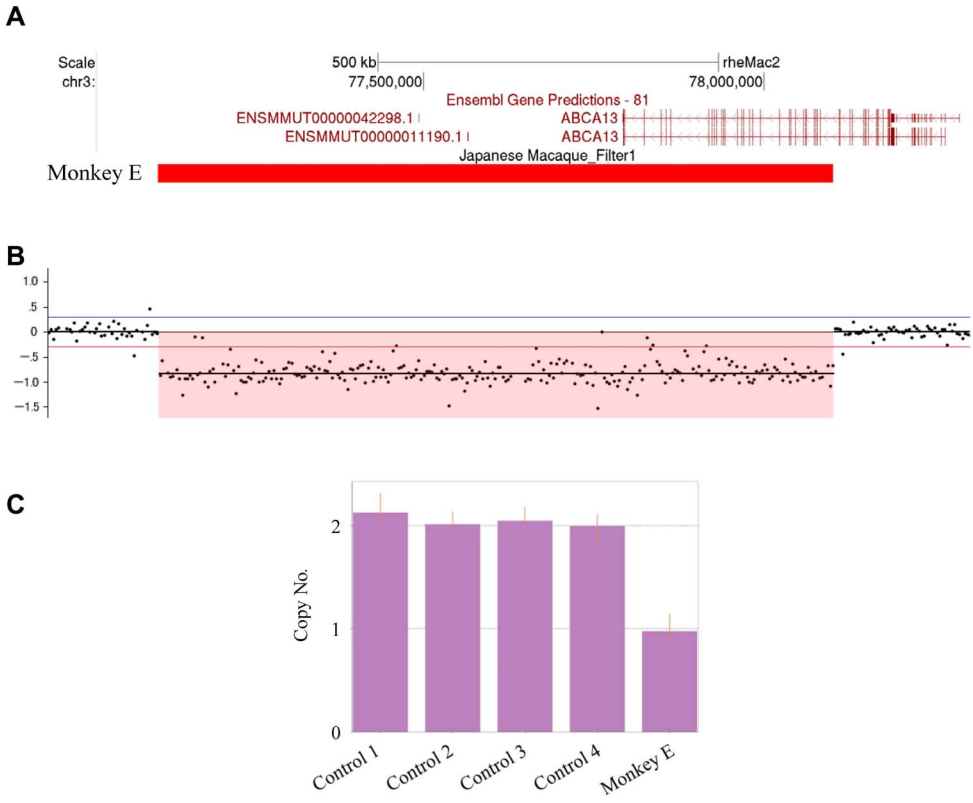

Fig. 5. Rare deletion disrupting *ABCA13* in monkey E. (**A**) Heterozygous *ABCA13* deletion in monkey E (red bar). The coordinates of the deletion were chr3:77110419-78101380, as determined on the basis of the rhesus macaque (*Macaca mulatta*) genome assembly (rheMac2, January 2006). Gene annotation was taken from Ensembl Gene Predictions (Ensembl 76). Two Ensembl transcripts (ENSMMUT00000011190 and ENSMMUT00000042298) overlapping this deletion were derived from pseudogenes. (**B**) Log2 ratio plot of *ABCA13* deletion. The data were obtained from aCGH results. (**C**) *ABCA13* deletion in monkey E was validated by a real-time PCR-based TaqMan copy number assay. Bars indicate copy numbers predicted by this assay. Controls 1 to 4 carried no aCGH-detected CNVs at *ABCA13* (copy number = 2).

traits may bear strong relevance to the hypothesis that autistic persons have dysfunctional mirror neuron systems (*31*), which is known as the "broken mirror hypothesis" (*32*). Mirror neurons are a class of neurons originally found in the monkey ventral premotor cortex (PMv) that respond to both one's own actions and those of others (*33*). These neurons are also hypothesized to receive visual information about others' actions from the STS via the inferior parietal lobule (IPL) (*34*, *35*). From the similarity between the function impaired in ASD and proposed functional roles of mirror neurons (*35*), researchers hypothesize that early developmental failures of mirror neurons may result in the expression of behavioral disorders in ASD, an idea which is supported by numerous studies (*17*, *36*–*39*). For example, the suppression of the μ frequency (8 to 13 Hz) oscillation over the sensorimotor cortex, which is considered to reflect mirror neuron activity (*40*), occurs in response to both one's own movements and those of others in typically developing children (*17*), whereas this suppression occurs only during one's own movements in individuals with ASD (*17*, *39*).

Although there is abundant support for the broken mirror hypothesis in human subjects, direct cellular evidence has not been obtained—that is, evidence showing the paucity or dysfunction of classically defined mirror neurons in autistic states (these changes should be detected in the PMv or IPL). The main reason that this direct cellular evidence does not exist is the lack of nonhuman primate models of ASD, except for one representing symptomatic ASD (*41*). Here, we have shown that cortical neurons responsive to others' actions were virtually absent in the monkey with autistic traits, although recordings were made in the mentalizing system. Our study is on a single animal, and with all the findings above, we still need to be cautious in assuming it to be a spontaneous model of ASD. However, it would be interesting to hypothesize that aberrant processing of others' actions in the STS, as discussed above, results in the paucity of mirror- and partner-type neurons in the mentalizing system, as well as mirror neurons in the mirror system. This atypical cellular population in social brain networks may be associated with the emergence of behavioral disorders in ASD. It has been shown in neurotypical monkeys that neurons in the mirror system (IPL) are sensitive to the chained organization of others' actions (*42*); neurons in the mentalizing system (MFC) are associated with the organization of one's own actions in socially adaptive manners (*5*) and the prediction of others' internal processes (*43*). These behavioral aspects are disrupted in people with ASD (*44*, *45*). An important step for future work will be to determine whether the genetic variants in *ABCA13* and *HTR2C* preferentially affect the STS and/or its projections to the IPL and MFC.

The availability of whole-genome sequences at the individual level has now enabled researchers to create a new discipline called cognitive genomics. To date, cognitive genomics research in monkeys has taken

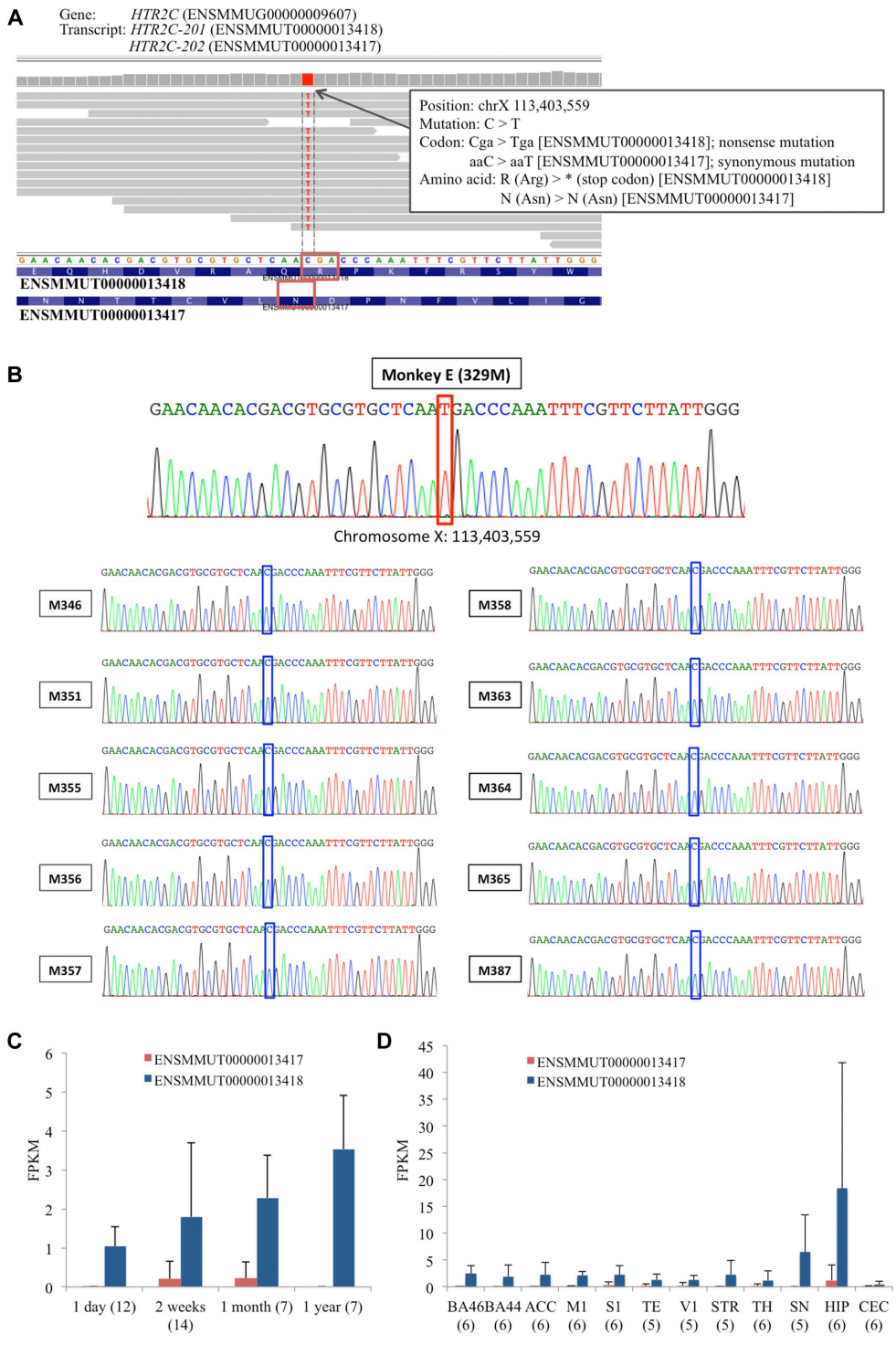

Fig. 6. Nonsense mutation affecting *HTR2C* in monkey E. (**A**) Alignment of short-read sequences on *HTR2C* showing cytosine-to-thymine mutation. This mutation affected the truncated isoforms (*HTR002_001*: ENSMMUT00000013418), conferring nonsense mutation on this isoform. (**B**) Sanger-based sequencing for genotyping *HTR2C* mutation. PCR was performed in monkey E (top) and 10 other male monkeys as controls. The result indicates that only monkey E has the LoF mutation (C-to-T mutation) at the position of 113,403,559 on chromosome X, and all other control monkeys show wild-type genotypes at the same position. (**C** and **D**) Expression levels of two *HTC2C* isoforms in a series of developmental stages (C) and in different brain regions (D). Values in parentheses represent the number of samples. Error bars represent SEM. FPKM, fragments per kilobase of exon per million fragments mapped; BA46, Brodmann area 46; BA44, Brodmann area 44; ACC, anterior cingulate cortex; M1, primary motor cortex; S1, primary somatosensory cortex; TE, inferior temporal gyrus; V1, primary visual cortex; STR, striatum; TH, thalamus; SN, substantia nigra; HIP, hippocampus; CEC, cerebellum.

a "genotype-first" approach—an attempt to determine how cognition and behavior can differ between individuals depending on polymorphisms of a specific target gene (*46*–*49*). This study is the first demonstration of the inverse, "phenotype-first" approach, where an attempt to identify genetic correlates of atypical social behavior was made. Generally, monkeys with unusual cognitive traits are not considered suitable for use in basic physiological research. Here, we propose to closely examine these monkeys, from the behavioral to the neuronal and genetic levels, rather than excluding them as research subjects. We expect that our approach that combines systems neuroscience and cognitive genomics in macaques, along with a transgenic approach (*41*), will contribute to the clarification of biological mechanisms underlying neuropsychiatric disorders.

MATERIALS AND METHODS

Subjects for behavioral and electrophysiological experiments

We used three male Japanese macaques (*M. fuscata*; designated as N, S, and E). The monkeys were housed in individual cages. T1-weighted structural brain magnetic resonance images were obtained using a 4-T Varian Unity Inova system (Varian NMR Instruments); no apparent abnormality was detected in any of the three monkeys. All procedures for animal care and experimentation were approved by the Animal Experiment Committee of RIKEN and complied with the Public Health Service Policy on the Humane Care and Use of Laboratory Animals (http://grants.nih.gov/grants/olaw/references/phspol.htm).

Behavioral procedures: Role-reversal task

The monkeys were trained to perform a role-reversal task, as described previously (*5*, *10*), in three different pairs (N and E, N and S, and S and E). In each experimental session, two monkeys sitting in their individual primate chairs faced each other across a square table (60 cm × 60 cm) in a sound-attenuated room. Two sets of three white buttons were placed on the table; each set consisted of a start button and two target buttons, which were placed out of reach of the monkey on the other side (Fig. 1A). In each trial, one monkey was assigned the role of actor and the other monkey was assigned the role of observer. These two roles alternated every two trials (Fig. 1B). Each trial was designated as a self-trial or a partner's trial according to whether the actor was oneself or one's partner.

Each trial started when the start button at the actor's side turned red, which the actor had to press with its right hand. After 1 to 1.5 s, the start button turned off and, simultaneously, the two target buttons at the actor's side turned yellow and green (their positions changed randomly across trials). Then, the actor was required to press one of the target buttons within 3 s with its right hand. The observer was required to sit still with its right hand placed continuously on the start button throughout the trial.

During a block of 5 to 17 successive trials, a reward (isotonic water) was consistently associated with one target color (yellow or green; Fig. 1B). When the actor chose the correct target, both monkeys were rewarded 1.3 s after the target button was pressed. However, when the actor chose the wrong target, neither monkey was rewarded. The reward-associated color was then reversed in the next trial block without any external cue. Because of the unpredictability of block switches, the actor's choice in the first trial in each block ("switch trials"; see arrows in Fig. 1B) led to the omission of a reward in most cases (N, 99%; S, 96%; and E, 95%). Solenoid valves controlling the delivery of the reward were placed outside the sound-attenuated room. The task was controlled using a LabVIEW Real-Time system (National Instruments).

Behavioral analyses

First, we calculated the percentage of correct choice of each monkey when the previous and current trials were nonswitch ones and the choice in the previous trial was correct. As the roles alternated every two trials, the actor of the previous trial was either oneself or one's partner (Fig. 2A; see also Supplementary Text for the slightly lower percentage of correct choice of monkey E following its partner's trials).

Then, we analyzed the behavior after unrewarded trials. There were two different types of no-reward trial (*5*). The first type was no reward due to a block change. Because the color-reward association changed randomly without a signal, the monkeys could not predict when it would happen. Therefore, the first trial of each block usually ended in no reward, as described above. After this type of no-reward trial, the monkeys needed to switch their choice of color (Fig. 2B).

The second type was no reward due to a choice error. The monkeys occasionally happened to choose the wrong color in the middle of a block. After this type of no-reward trial, the monkeys should not switch their choice of color from that chosen in the trial before the error (Fig. 2C).

Furthermore, taking the factor of agent (self/other) into consideration, the no-reward trials were further classified into four types: choice error and error due to block change by either self or one's partner. We reasoned that if the monkeys coped with these four types differently, the RTs in the subsequent trials would vary. To test this possibility, we compared each monkey's RTs following four types of no-reward trial using one-way ANOVA, regardless of the result of the present choice (fig. S3).

Behavioral procedures: Food-grab task

In an attempt to determine social hierarchy between the monkeys, we carried out a food-grab task. In each trial, an experimenter placed a small piece of food (raisins or banana-flavored pellets) in front of two monkeys sitting face-to-face in their individual chairs. The food item was placed at a position equally distant from the monkeys. Then, the monkeys were allowed to grab it freely under the competitive context. Each session consisted of 10 trials. We counted the number of successful acquisitions by each monkey in each pair. An analysis revealed that monkey N obtained food items significantly more often when tested with monkeys S and E ($P = 0.031$ each; Wilcoxon signed-rank test). However, the success rate was not significantly different between monkeys S and E ($P = 1.0$). These findings suggest that monkey N was dominant over monkeys S and E, whereas no particular hierarchical order was established between monkeys S and E, at least under the task context.

Surgical procedures

A nonmetal post and chamber for head immobilization and neuronal recording, respectively, were fixed firmly on the skull using dental resin under general anesthesia and aseptic surgical conditions. The recording chamber was stereotaxically placed in the midline over the frontal cortex. The monkeys were administered antibiotics and analgesics following the surgery.

Behavioral and electrophysiological recording procedures

Single-unit recording was carried out in the MFC while the monkeys performed the role-reversal task. In each session, we recorded from one monkey. Extracellular potentials were obtained using tungsten electrodes with impedances of 0.5 to 1.0 megohms (Frederick Haer). Unit activity was amplified and band-pass–filtered (600 to 6000 Hz) using the Digital Lynx system (Neuralynx). An oil-driven micromanipulator (MO-971A; Narishige) was used to advance an electrode through a stainless steel guide tube that was held in place by a grid. The grid allowed neuronal recordings every 1 mm between penetrations. Single units were isolated offline using an offline sorter (Plexon). We sampled all easily isolable neurons.

The animals' horizontal and vertical eye positions were sampled at 250 Hz using an infrared corneal reflection system (EyeLink; SR Research). The locations of the target buttons were mapped empirically using the monkeys' recorded eye positions. Electromyographic activity was recorded (MEG-5100; Nihon Kohden) from the following limb and trunk muscles in monkey N: anterior deltoid, biceps brachii, triceps brachii, pectoralis major, upper trapezius, and latissimus dorsi.

Cortical recording sites

Neuronal recordings were carried out in two cortical subregions, that is, the dorsomedial convexity subregion (MFC convexity) and the cingulate sulcus subregion (MFC sulcus). The MFC convexity mainly included the pre-SMA (see below for the definition) and prefrontal area 9 (*8*) immediately rostral to the pre-SMA. The MFC sulcus was contained in the dorsal bank and fundus of the cingulate sulcus. It largely corresponded to the rostral cingulate motor area (*9*) and its rostrally adjacent prefrontal region (area 24c). Both subregions were searched primarily on the left side with the aid of magnetic resonance images.

In the MFC convexity, we first mapped the border between the SMA and pre-SMA in accordance with the physiological criteria established previously (*50*). Specifically, we mapped the forelimb representation of the SMA on the basis of motor effects evoked by intracortical microstimulation (ICMS; cathodal pulses of 0.2 ms duration at 333 Hz), as well as consistent, neuronal responses to somatosensory stimulation applied to the contralateral forelimb. In the SMA, brisk movements involving a single joint were elicitable on the contralateral side with 12 to 22 pulses at a current intensity lower than 40 μA. We then mapped the face representation of the SMA just rostrally to the forelimb representation. The face-representing region typically spanned 1 to 2 mm in the rostrocaudal dimension. Finally, we identified the pre-SMA just rostrally to the face representation of the SMA. In the pre-SMA, somatosensory responses were less frequent and less consistent. Moreover, ICMS with ≥40 pulses and ≥40 μA was usually required to elicit forelimb movements.

Neuronal data analysis

We quantified the firing rate of each neuron during an action period, defined as a 200-ms duration before the actor pressed the correct target button. The activity in this period could be selective for or influenced by the following four factors: agent (self or partner), target location (right or left), target color (yellow or green), and trial position within the actor's turns in a row (first or second). We therefore performed a four-way ANOVA to test the effect of these factors on neuronal activity ($\alpha = 0.01$).

A neuron was defined to be of the self type when it showed a significant main effect of agent (self-trials > partner trials) and also when its activity in the action period was significantly higher than that in the control period (200 to 0 ms before target onset) in self-trials ($P < 0.01$, Wilcoxon signed-rank test). Likewise, a neuron was defined to be of the partner type when it showed a significant main effect of agent (partner trials > self-trials) and also when its activity in the action period was significantly greater than that in the control period in partner trials. Finally, a neuron was defined to be of the mirror type when it lacked a significant main effect of agent and also when the discharge rate in the action period was significantly higher than that in the control period in both self- and partner trials. All statistical analyses were assessed by two-tailed tests using MATLAB (MathWorks).

Procedures for CNV analysis

Peripheral blood was collected from 336 Japanese macaques (*M. fuscata*), including monkeys N, S, and E. Genomic DNA was then extracted using standard protocol.

We designed oligonucleotide arrays on the basis of the reference genome sequence of the rhesus macaque (*M. mulatta*) genome assembly (rheMac2, January 2006) provided by NimbleGen Systems Inc. The custom-made arrays contained 720,000 probes with an average probe spacing of 4.0 kb throughout the genome. aCGH was performed according to the manufacturer's instructions. Reference DNA from a pool of five individuals was used for sex-matched controls. Then, high-resolution custom-made arrays containing 2,100,000 probes (with an average probe spacing of 1.4 kb) were used to validate *ABCA13* deletion.

CNV calls were made with Nexus Copy Number software version 7.5 (BioDiscovery) using the Fast Adaptive States Segmentation Technique 2 algorithm, which is a hidden Markov model–based approach. To obtain high-confidence CNV calls, stringent log 2 ratio thresholds were set for loss and gain based on CNV size: (i) CNV ≥ 500 kb, <−0.4 for deletions and >0.3 for duplications; (ii) 100 kb ≤ CNV < 500 kb, <−0.6 for deletions and >0.4 for duplications; and (iii) 10 kb ≤ CNV < 100 kb, <−0.7 for deletions and >0.45 for duplications. The significance threshold P value was set at 1×10^{-9}, and at least five contiguous probes were required for CNV calls. A noise-reduction algorithm for aCGH data was used as a systematic correction of artifacts caused by GC content and fragment length (*51*). Quality control (QC) scores were calculated for each sample on the basis of the statistical variance of the probe-to-probe log ratios. We removed samples with QC >0.15 or with ≥46 CNVs (outliers). Then, we excluded CNVs <10 kb and those with low probe densities (<1 probe/15 kb). All genomic locations are given in the rhesus macaque (*M. mulatta*) genome assembly (rheMac2, January 2006). Gene annotation was based on Ensembl Gene Predictions (Ensembl 76).

Procedures for CNV validation

A real-time PCR-based TaqMan copy number assay (Applied Biosystems) was performed to validate *ABCA13* deletion in monkey E. A FAM (6-carboxyfluorescein)–labeled test assay was selected from the deletion region and a VIC (4,7,2′-trichloro-7′-phenyl-6-carboxyfluorescein)–labeled reference assay was selected from the ribonuclease (RNase) P region. The experiment was performed in quadruplicate, multiplexed 10-μl reactions containing TaqMan Universal PCR Master Mix, the VIC-labeled RNase P reference assay, and the FAM-labeled

test assay. Samples with normal copy number were used to calibrate each assay. Reactions were performed in 384-well plates on the ABI 7900HT Real-Time PCR System (Applied Biosystems), and data were collected with SDS version 2.4 (Applied Biosystems). Data were analyzed with a manual Ct threshold of 0.2, and an automatic baseline and copy numbers were determined using the CopyCaller software (Applied Biosystems).

Procedures for exome analysis, Sanger-sequencing, and messenger RNA sequencing

Extensive exon sequencing (known as exome) approaches were performed in 100 macaques, including monkeys N, S, and E (78 Japanese macaques, *M. fuscata*; 22 rhesus macaques, *M. mulatta*) with the Next-Generation Sequencer of HiSeq2000 (Illumina Inc.). Specifically, using human whole-exon capture probes (TruSeq Exome Enrichment Kit, Illumina Inc.), 62 Mb of all exon regions was sequenced. We trimmed adapter sequences and low-quality bases and mapped them to rheMac2 using bowtie2 (*52*). Downstream analyses for variant calling were performed using SAMtools (*53*), Picard Tools (http://broadinstitute.github.io/picard/), and GATK (Genome Analysis Toolkit) software tools (*54*, *55*). SnpEff (version 3.3) was used to annotate all variants and their potential mutational effects on associated transcripts (*56*), and the LoF mutations, such as splice acceptor/donor site mutations, start codon lost mutations, and stop codon gained/lost mutations, were obtained. Gene annotation was based on Ensembl Gene Predictions (Ensembl 78).

Additionally, Sanger-based sequencing was performed to confirm the LoF mutation in monkey E and 10 other monkeys as controls using the following primers: TGCCGTGAATAGCTTTCAACA (forward primer) and TCGGCGAAGAACGTAGATCG (reverse primer). PCR amplification was performed using the following conditions: initial denaturation at 98°C for 2 min, 35 cycles of denaturation at 98°C for 10 s, annealing at 60°C for 30 s, and extension at 72°C for 5 s, followed by a final extension at 72°C for 4 min.

Messenger RNA sequencing data were generated from four developmental stages (1 day, 2 weeks, 1 month, and 1 year) and 12 brain regions [Brodmann area 46, Brodmann area 44, anterior cingulate cortex (including the MFC sulcus), primary motor cortex, primary somatosensory cortex, inferior temporal gyrus, primary visual cortex, striatum, thalamus, substantia nigra, hippocampus, and cerebellum]. Libraries were prepared using an Illumina TruSeq RNA Library Prep Kit and sequenced in the 50-bp single-end mode using Illumina HiSeq2000. Sequencing reads were mapped using TopHat2 (*57*) on rheMac2. Genome-wide expression levels were measured as a unit of fragments per kilobase of exon per million fragments mapped using Cufflinks (*58*), and the relative expression levels of *HTR2C* isoforms were determined using Cuffdiff pipeline implemented into Cufflinks.

SUPPLEMENTARY MATERIALS

Supplementary material for this article is available at http://advances.sciencemag.org/cgi/content/full/2/9/e1600558/DC1

Supplementary Text

fig. S1. Effects of outcomes in two trials before current choice.

fig. S2. Animals' gaze behavior.

fig. S3. Animals' RT analysis.

fig. S4. Three types of agent-related neurons in the MFC.

table S1. All CNVs detected in monkey E.

table S2. All LoF mutations only identified in monkey E.

References (*59*–*100*)

REFERENCES AND NOTES

1. American Psychiatric Association, *Diagnostic and Statistical Manual of Mental Disorders* (American Psychiatric Publishing, Arlington, VA, ed. 5, 2013).
2. J. Nakatani, K. Tamada, F. Hatanaka, S. Ise, H. Ohta, K. Inoue, S. Tomonaga, Y. Watanabe, Y. J. Chung, R. Banerjee, K. Iwamoto, T. Kato, M. Okazawa, K. Yamauchi, K. Tanda, K. Takao, T. Miyakawa, A. Bradley, T. Takumi, Abnormal behavior in a chromosome-engineered mouse model for human 15q11-13 duplication seen in autism. *Cell* **137**, 1235–1246 (2009).
3. C. D. Frith, U. Frith, Interacting minds—A biological basis. *Science* **286**, 1692–1695 (1999).
4. F. Van Overwalle, K. Baetens, Understanding others' actions and goals by mirror and mentalizing systems: A meta-analysis. *Neuroimage* **48**, 564–584 (2009).
5. K. Yoshida, N. Saito, A. Iriki, M. Isoda, Social error monitoring in macaque frontal cortex. *Nat. Neurosci.* **15**, 1307–1312 (2012).
6. S. Baron-Cohen, Autism: The empathizing–systemizing (E-S) theory. *Ann. N. Y. Acad. Sci.* **1156**, 68–80 (2009).
7. M. V. Lombardo, B. Chakrabarti, E. T. Bullmore, S. A. Sadek, G. Pasco, S. J. Wheelwright, J. Suckling; MRC AIMS Consortium, S. Baron-Cohen, Atypical neural self-representation in autism. *Brain* **133**, 611–624 (2010).
8. H. Barbas, D. N. Pandya, Architecture and intrinsic connections of the prefrontal cortex in the rhesus monkey. *J. Comp. Neurol.* **286**, 353–375 (1989).
9. R. P. Dum, P. L. Strick, The origin of corticospinal projections from the premotor areas in the frontal lobe. *J. Neurosci.* **11**, 667–689 (1991).
10. K. Yoshida, N. Saito, A. Iriki, M. Isoda, Representation of others' action by neurons in monkey medial frontal cortex. *Curr. Biol.* **21**, 249–253 (2011).
11. M. Tomioka, Y. Toda, J. Kurisu, Y. Kimura, M. Kengaku, K. Ueda, The effects of neurological disorder-related codon variations of ABCA13 on the function of the ABC protein. *Biosci. Biotechnol. Biochem.* **76**, 2289–2293 (2012).
12. H. M. Knight, B. S. Pickard, A. Maclean, M. P. Malloy, D. C. Soares, A. F. McRae, A. Condie, A. White, W. Hawkins, K. McGhee, M. van Beck, D. J. MacIntyre, J. M. Starr, I. J. Deary, P. M. Visscher, D. J. Porteous, R. E. Cannon, D. St Clair, W. J. Muir, Douglas H. R. Blackwood, A cytogenetic abnormality and rare coding variants identify *ABCA13* as a candidate gene in schizophrenia, bipolar disorder, and depression. *Am. J. Hum. Genet.* **85**, 833–846 (2009).
13. I. Iossifov, M. Ronemus, D. Levy, Z. Wang, I. Hakker, J. Rosenbaum, B. Yamrom, Y.-H. Lee, G. Narzisi, A. Leotta, J. Kendall, E. Grabowska, B. Ma, S. Marks, L. Rodgers, A. Stepansky, J. Troge, P. Andrews, M. Bekritsky, K. Pradhan, E. Ghiban, M. Kramer, J. Parla, R. Demeter, L. L. Fulton, R. S. Fulton, V. J. Magrini, K. Ye, J. C. Darnell, R. B. Darnell, E. R. Mardis, R. K. Wilson, M. C. Schatz, W. R. McCombie, M. Wigler, De novo gene disruptions in children on the autistic spectrum. *Neuron* **74**, 285–299 (2012).
14. B. M. Neale, Y. Kou, L. Liu, A. Ma'ayan, K. E. Samocha, A. Sabo, C.-F. Lin, C. Stevens, L.-S. Wang, V. Makarov, P. Polak, S. Yoon, J. Maguire, E. L. Crawford, N. G. Campbell, E. T. Geller, O. Valladares, C. Schafer, H. Liu, T. Zhao, G. Cai, J. Lihm, R. Dannenfelser, O. Jabado, Z. Peralta, U. Nagaswamy, D. Muzny, J. G. Reid, I. Newsham, Y. Wu, L. Lewis, Y. Han, B. F. Voight, E. Lim, E. Rossin, A. Kirby, J. Flannick, M. Fromer, K. Shakir, T. Fennell, K. Garimella, E. Banks, R. Poplin, S. Gabriel, M. DePristo, J. R. Wimbish, B. E. Boone, S. E. Levy, C. Betancur, S. Sunyaev, E. Boerwinkle, J. D. Buxbaum, E. H. Cook Jr., B. Devlin, R. A. Gibbs, K. Roeder, G. D. Schellenberg, J. S. Sutcliffe, M. J. Daly, Patterns and rates of exonic de novo mutations in autism spectrum disorders. *Nature* **485**, 242–245 (2012).
15. C. M. Niswender, K. Herrick-Davis, G. E. Dilley, H. Y. Meltzer, J. C. Overholser, C. A. Stockmeier, R. B. Emeson, E. Sanders-Bush, RNA editing of the human serotonin 5-HT_{2C} receptor. alterations in suicide and implications for serotonergic pharmacotherapy. *Neuropsychopharmacology* **24**, 478–491 (2001).
16. B. Lerer, F. Macciardi, R. H. Segman, R. Adolfsson, D. Blackwood, S. Blairy, J. Del Favero, D. G. Dikeos, R. Kaneva, R. Lilli, I. Massat, V. Milanova, W. Muir, M. Noethen, L. Oruc, T. Petrova, G. N. Papadimitriou, M. Rietschel, A. Serretti, D. Souery, S. Van Gestel, C. Van Broeckhoven, J. Mendlewicz, Variability of 5-HT2C receptor cys23ser polymorphism among European populations and vulnerability to affective disorder. *Mol. Psychiatry* **6**, 579–585 (2001).
17. L. M. Oberman, E. M. Hubbard, J. P. McCleery, E. L. Altschuler, V. S. Ramachandran, J. A. Pineda, EEG evidence for mirror neuron dysfunction in autism spectrum disorders. *Brain Res. Cogn. Brain Res.* **24**, 190–198 (2005).
18. G. Luppino, R. Calzavara, S. Rozzi, M. Matelli, Projections from the superior temporal sulcus to the agranular frontal cortex in the macaque. *Eur. J. Neurosci.* **14**, 1035–1040 (2001).
19. T. Allison, A. Puce, G. McCarthy, Social perception from visual cues: Role of the STS region. *Trends Cogn. Sci.* **4**, 267–278 (2000).
20. A. Puce, T. Allison, S. Bentin, J. C. Gore, G. McCarthy, Temporal cortex activation in humans viewing eye and mouth movements. *J. Neurosci.* **18**, 2188–2199 (1998).
21. D. I. Perrett, P. A. Smith, A. J. Mistlin, A. J. Chitty, A. S. Head, D. D. Potter, R. Broennimann, A. D. Milner, M. A. Jeeves, Visual analysis of body movements by neurones in the temporal cortex of the macaque monkey: A preliminary report. *Behav. Brain Res.* **16**, 153–170 (1985).

22. D. I. Perrett, M. H. Harries, R. Bevan, S. Thomas, P. J. Benson, A. J. Mistlin, A. J. Chitty, J. K. Hietanen, J. E. Ortega, Frameworks of analysis for the neural representation of animate objects and actions. *J. Exp. Biol.* **146**, 87–113 (1989).
23. T. Jellema, C. I. Baker, B. Wicker, D. I. Perrett, Neural representation for the perception of the intentionality of hand actions. *Brain Cogn.* **44**, 280–302 (2001).
24. S. Dakin, U. Frith, Vagaries of visual perception in autism. *Neuron* **48**, 497–507 (2005).
25. M. Zilbovicius, I. Meresse, N. Chabane, F. Brunelle, Y. Samson, N. Boddaert, Autism, the superior temporal sulcus and social perception. *Trends Neurosci.* **29**, 359–366 (2006).
26. N. Boddaert, N. Chabane, H. Gervais, C. D. Good, M. Bourgeois, M.-H. Plumet, C. Barthélémy, M.-C. Mouren, E. Artiges, Y. Samson, F. Brunelle, R. S. J. Frackowiak, M. Zilbovicius, Superior temporal sulcus anatomical abnormalities in childhood autism: A voxel-based morphometry MRI study. *Neuroimage* **23**, 364–369 (2004).
27. M. Zilbovicius, N. Boddaert, P. Belin, J.-B. Poline, P. Remy, J.-F. Mangin, L. Thivard, C. Barthélémy, Y. Samson, Temporal lobe dysfunction in childhood autism: A PET study. Positron emission tomography. *Am. J. Psychiatry* **157**, 1988–1993 (2000).
28. T. Ohnishi, H. Matsuda, T. Hashimoto, T. Kunihiro, M. Nishikawa, T. Uema, M. Sasaki, Abnormal regional cerebral blood flow in childhood autism. *Brain* **123**, 1838–1844 (2000).
29. I. G. Meresse, M. Zilbovicius, N. Boddaert, L. Robel, A. Philippe, I. Sfaello, L. Laurier, F. Brunelle, Y. Samson, M.-C. Mouren, N. Chabane, Autism severity and temporal lobe functional abnormalities. *Ann. Neurol.* **58**, 466–469 (2005).
30. F. Castelli, C. Frith, F. Happé, U. Frith, Autism, Asperger syndrome and brain mechanisms for the attribution of mental states to animated shapes. *Brain* **125** (Pt. 8), 1839–1849 (2002).
31. J. H. G. Williams, A. Whiten, T. Suddendorf, D. I. Perrett, Imitation, mirror neurons and autism. *Neurosci. Biobehav. Rev.* **25**, 287–295 (2001).
32. V. S. Ramachandran, L. M. Oberman, Broken mirrors: A theory of autism. *Sci. Am.* **295**, 62–69 (2006).
33. G. di Pellegrino, L. Fadiga, L. Fogassi, V. Gallese, G. Rizzolatti, Understanding motor events: A neurophysiological study. *Exp. Brain Res.* **91**, 176–180 (1992).
34. G. Rizzolatti, G. Luppino, The cortical motor system. *Neuron* **31**, 889–901 (2001).
35. G. Rizzolatti, M. Fabbri-Destro, Mirror neurons: From discovery to autism. *Exp. Brain Res.* **200**, 223–237 (2010).
36. N. Nishitani, S. Avikainen, R. Hari, Abnormal imitation-related cortical activation sequences in Asperger's syndrome. *Ann. Neurol.* **55**, 558–562 (2004).
37. H. Théoret, E. Halligan, M. Kobayashi, F. Fregni, H. Tager-Flusberg, A. Pascual-Leone, Impaired motor facilitation during action observation in individuals with autism spectrum disorder. *Curr. Biol.* **15**, R84–R85 (2005).
38. M. Dapretto, M. S. Davies, J. H. Pfeifer, A. A. Scott, M. Sigman, S. Y. Bookheimer, M. Iacoboni, Understanding emotions in others: Mirror neuron dysfunction in children with autism spectrum disorders. *Nat. Neurosci.* **9**, 28–30 (2006).
39. J. Martineau, S. Cochin, R. Magne, C. Barthelemy, Impaired cortical activation in autistic children: Is the mirror neuron system involved? *Int. J. Psychophysiol.* **68**, 35–40 (2008).
40. S. D. Muthukumaraswamy, B. W. Johnson, N. A. McNair, Mu rhythm modulation during observation of an object-directed grasp. *Brain Res. Cogn. Brain Res.* **19**, 195–201 (2004).
41. Z. Liu, X. Li, J.-T. Zhang, Y.-J. Cai, T.-L. Cheng, C. Cheng, Y. Wang, C.-C. Zhang, Y.-H. Nie, Z.-F. Chen, W.-J. Bian, L. Zhang, J. Xiao, B. Lu, Y.-F. Zhang, X.-D. Zhang, X. Sang, J.-J. Wu, X. Xu, Z.-Q. Xiong, F. Zhang, X. Yu, N. Gong, W.-H. Zhou, Q. Sun, Z. Qiu, Autism-like behaviours and germline transmission in transgenic monkeys overexpressing MeCP2. *Nature* **530**, 98–102 (2016).
42. L. Fogassi, P. F. Ferrari, B. Gesierich, S. Rozzi, F. Chersi, G. Rizzolatti, Parietal lobe: From action organization to intention understanding. *Science* **308**, 662–667 (2005).
43. K. Haroush, Z. M. Williams, Neuronal prediction of opponent's behavior during cooperative social interchange in primates. *Cell* **160**, 1233–1245 (2015).
44. L. Cattaneo, M. Fabbri-Destro, S. Boria, C. Pieraccini, A. Monti, G. Cossu, G. Rizzolatti, Impairment of actions chains in autism and its possible role in intention understanding. *Proc. Natl. Acad. Sci. U.S.A.* **104**, 17825–17830 (2007).
45. S. Baron-Cohen, A. M. Leslie, U. Frith, Does the autistic child have a "theory of mind"? *Cognition* **21**, 37–46 (1985).
46. A. Izquierdo, T. K. Newman, J. D. Higley, E. A. Murray, Genetic modulation of cognitive flexibility and socioemotional behavior in rhesus monkeys. *Proc. Natl. Acad. Sci. U.S.A.* **104**, 14128–14133 (2007).
47. K. K. Watson, J. H. Ghodasra, M. L. Platt, Serotonin transporter genotype modulates social reward and punishment in rhesus macaques. *PLOS One* **4**, e4156 (2009).
48. G.-L. Chen, M. A. Novak, J. S. Meyer, B. J. Kelly, E. J. Vallender, G. M. Miller, The effect of rearing experience and TPH2 genotype on HPA axis function and aggression in rhesus monkeys: A retrospective analysis. *Horm. Behav.* **57**, 184–191 (2010).
49. L. J. N. Brent, S. R. Heilbronner, J. E. Horvath, J. Gonzalez-Martinez, A. Ruiz-Lambides, A. G. Robinson, J. H. P. Skene, M. L. Platt, Genetic origins of social networks in rhesus macaques. *Sci. Rep.* **3**, 1042 (2013).
50. Y. Matsuzaka, H. Aizawa, J. Tanji, A motor area rostral to the supplementary motor area (presupplementary motor area) in the monkey: Neuronal activity during a learned motor task. *J. Neurophysiol.* **68**, 653–662 (1992).
51. F. Leprêtre, C. Villenet, S. Quief, O. Nibourel, C. Jacquemin, X. Troussard, F. Jardin, F. Gibson, J. P. Kerckaert, C. Roumier, M. Figeac, Waved aCGH: To smooth or not to smooth. *Nucleic Acids Res.* **38**, e94 (2010).
52. B. Langmead, S. L. Salzberg, Fast gapped-read alignment with Bowtie 2. *Nat. Methods* **9**, 357–359 (2012).
53. H. Li, B. Handsaker, A. Wysoker, T. Fennell, J. Ruan, N. Homer, G. Marth, G. Abecasis, R. Durbin; Genome Project Data Processing Subgroup, The Sequence Alignment/Map format and SAMtools. *Bioinformatics* **25**, 2078–2079 (2009).
54. A. McKenna, M. Hanna, E. Banks, A. Sivachenko, K. Cibulskis, A. Kernytsky, K. Garimella, D. Altshuler, S. Gabriel, M. Daly, M. A. DePristo, The Genome Analysis Toolkit: A MapReduce framework for analyzing next-generation DNA sequencing data. *Genome Res.* **20**, 1297–1303 (2010).
55. M. A. DePristo, E. Banks, R. Poplin, K. V. Garimella, J. R. Maguire, C. Hartl, A. A. Philippakis, G. del Angel, M. A. Rivas, M. Hanna, A. McKenna, T. J. Fennell, A. M. Kernytsky, A. Y. Sivachenko, K. Cibulskis, S. B. Gabriel, D. Altshuler, M. J. Daly, A framework for variation discovery and genotyping using next-generation DNA sequencing data. *Nat. Genet.* **43**, 491–498 (2011).
56. P. Cingolani, A. Platts, L. L. Wang, M. Coon, T. Nguyen, L. Wang, S. J. Land, X. Lu, D. M. Ruden, A program for annotating and predicting the effects of single nucleotide polymorphisms, SnpEff: SNPs in the genome of *Drosophila melanogaster* strain w^{1118}; iso-2; iso-3. *Fly* **6**, 80–92 (2012).
57. C. Trapnell, L. Pachter, S. L. Salzberg, TopHat: Discovering splice junctions with RNA-Seq. *Bioinformatics* **25**, 1105–1111 (2009).
58. C. Trapnell, B. A. Williams, G. Pertea, A. Mortazavi, G. Kwan, M. J. van Baren, S. L. Salzberg, B. J. Wold, L. Pachter, Transcript assembly and quantification by RNA-Seq reveals unannotated transcripts and isoform switching during cell differentiation. *Nat. Biotechnol.* **28**, 511–515 (2010).
59. C. Prades, C. Prades, I. Arnould, T. Annilo, S. Shulenin, Z. Q. Chen, L. Orosco, M. Triunfol, C. Devaud, C. Maintoux-Larois, C. Lafargue, C. Lemoine, P. Denèfle, M. Rosier, M. Dean, The human ATP binding cassette gene ABCA13, located on chromosome 7p12.3, encodes a 5058 amino acid protein with an extracellular domain encoded in part by a 4.8-kb conserved exon. *Cytogenet. Genome Res.* **98**, 160–168 (2002).
60. C. Albrecht, E. Viturro, The ABCA subfamily–Gene and protein structures, functions and associated hereditary diseases. *Pflugers Arch.* **453**, 581–589 (2007).
61. N. Wang, D. L. Silver, P. Costet, A. R. Tall, Specific binding of ApoA-I, enhanced cholesterol efflux, and altered plasma membrane morphology in cells expressing ABC1. *J. Biol. Chem.* **275**, 33053–33058 (2000).
62. S. Beharry, M. Zhong, R. S. Molday, *N*-retinylidene-phosphatidylethanolamine is the preferred retinoid substrate for the photoreceptor-specific ABC transporter ABCA4 (ABCR). *J. Biol. Chem.* **279**, 53972–53979 (2004).
63. N. Wang, D. Lan, M. Gerbod-Giannone, P. Linsel-Nitschke, A. W. Jehle, W. Chen, L. O. Martinez, A. R. Tall, ATP-binding cassette transporter A7 (ABCA7) binds apolipoprotein A-I and mediates cellular phospholipid but not cholesterol efflux. *J. Biol. Chem.* **278**, 42906–42912 (2003).
64. M. Akiyama, Y. Sugiyama-Nakagiri, K. Sakai, J. R. McMillan, M. Goto, K. Arita, Y. Tsuji-Abe, N. Tabata, K. Matsuoka, R. Sasaki, D. Sawamura, H. Shimizu, Mutations in lipid transporter ABCA12 in harlequin ichthyosis and functional recovery by corrective gene transfer. *J. Clin. Invest.* **115**, 1777–1784 (2005).
65. A. Schmitt, K. Wilczek, K. Blennow, A. Maras, A. Jatzko, G. Petroianu, D. F. Braus, W. F. Gattaz, Altered thalamic membrane phospholipids in schizophrenia: A postmortem study. *Biol. Psychiatry* **56**, 41–45 (2004).
66. K. L. Davis, D. G. Stewart, J. I. Friedman, M. Buchsbaum, P. D. Harvey, P. R. Hof, J. Buxbaum, V. Haroutunian, White matter changes in schizophrenia: Evidence for myelin-related dysfunction. *Arch. Gen. Psychiatry* **60**, 443–456 (2003).
67. Y. Hakak, J. R. Walker, C. Li, W. H. Wong, K. L. Davis, J. D. Buxbaum, V. Haroutunian, A. A. Fienberg, Genome-wide expression analysis reveals dysregulation of myelination-related genes in chronic schizophrenia. *Proc. Natl. Acad. Sci. U.S.A.* **98**, 4746–4751 (2001).
68. D. Tkachev, M. L. Mimmack, M. M. Ryan, M. Wayland, T. Freeman, P. B. Jones, M. Starkey, M. J. Webster, R. H. Yolken, S. Bahn, Oligodendrocyte dysfunction in schizophrenia and bipolar disorder. *Lancet* **362**, 798–805 (2003).
69. S. Dracheva, K. L. Davis, B. Chin, D. A. Woo, J. Schmeidler, V. Haroutunian, Myelin-associated mRNA and protein expression deficits in the anterior cingulate cortex and hippocampus in elderly schizophrenia patients. *Neurobiol. Dis.* **21**, 531–540 (2006).
70. P. Katsel, K. L. Davis, V. Haroutunian, Variations in myelin and oligodendrocyte-related gene expression across multiple brain regions in schizophrenia: A gene ontology study. *Schizophr. Res.* **79**, 157–173 (2005).
71. P. R. Hof, V. Haroutunian, V. L. Friedrich Jr., W. Byne, C. Buitron, D. P. Perl, K. L. Davis, Loss and altered spatial distribution of oligodendrocytes in the superior frontal gyrus in schizophrenia. *Biol. Psychiatry* **53**, 1075–1085 (2003).
72. E. Tierney, N. A. Nwokoro, F. D. Porter, L. S. Freund, J. K. Ghuman, R. I. Kelley, Behavior phenotype in the RSH/Smith-Lemli-Opitz syndrome. *Am. J. Med. Genet.* **98**, 191–200 (2001).

73. D. M. Sikora, K. Pettit-Kekel, J. Penfield, L. S. Merkens, R. D. Steiner, The near universal presence of autism spectrum disorders in children with Smith–Lemli–Opitz syndrome. *Am. J. Med. Genet. A* **140**, 1511–1518 (2006).
74. S. Vancassel, G. Durand, C. Barthélémy, B. Lejeune, J. Martineau, D. Guilloteau, C. Andrès, S. Chalon, Plasma fatty acid levels in autistic children. *Prostaglandins Leukot. Essent. Fatty Acids* **65**, 1–7 (2001).
75. M. Maekawa, Y. Iwayama, R. Arai, K. Nakamura, T. Ohnishi, T. Toyota, M. Tsujii, Y. Okazaki, N. Osumi, Y. Owada, N. Mori, T. Yoshikawa, Polymorphism screening of brain-expressed *FABP7, 5* and *3* genes and association studies in autism and schizophrenia in Japanese subjects. *J. Hum. Genet.* **55**, 127–130 (2010).
76. A. Guilmatre, C. Dubourg, A.-L. Mosca, S. Legallic, A. Goldenberg, V. Drouin-Garraud, V. Layet, A. Rosier, S. Briault, F. Bonnet-Brilhault, F. Laumonnier, S. Odent, G. Le Vacon, G. Joly-Helas, V. David, C. Bendavid, J.-M. Pinoit, C. Henry, C. Impallomeni, E. Germano, G. Tortorella, G. Di Rosa, C. Barthelemy, C. Andres, L. Faivre, T. Frébourg, P. Saugier Veber, D. Campion, Recurrent rearrangements in synaptic and neurodevelopmental genes and shared biologic pathways in schizophrenia, autism, and mental retardation. *Arch. Gen. Psychiatry* **66**, 947–956 (2009).
77. J. P. H. Burbach, B. van der Zwaag, Contact in the genetics of autism and schizophrenia. *Trends Neurosci.* **32**, 69–72 (2009).
78. N. Craddock, M. J. Owen, The Kraepelinian dichotomy—Going, going… But still not gone. *Br. J. Psychiatry* **196**, 92–95 (2010).
79. Cross-Disorder Group of the Psychiatric Genomics Consortium, Identification of risk loci with shared effects on five major psychiatric disorders: A genome-wide analysis. *Lancet* **381**, 1371–1379 (2013).
80. D. Adam, Mental health: On the spectrum. *Nature* **496**, 416–418 (2013).
81. S. Collins, M. J. Lohse, B. O'Dowd, M. G. Caron, R. J. Lefkowitz, Structure and regulation of G protein-coupled receptors: The beta 2-adrenergic receptor as a model. *Vitam. Horm.* **46**, 1–39 (1991).
82. P. J. Conn, E. Sanders-Bush, B. J. Hoffman, P. R. Hartig, A unique serotonin receptor in choroid plexus is linked to phosphatidylinositol turnover. *Proc. Natl. Acad. Sci. U.S.A.* **83**, 4086–4088 (1986).
83. A. Pazos, D. Hoyer, J. M. Palacios, The binding of serotonergic ligands to the porcine choroid plexus: Characterization of a new type of serotonin recognition site. *Eur. J. Pharmacol.* **106**, 539–546 (1984).
84. S. M. Molineaux, T. M. Jessell, R. Axel, D. Julius, 5-HT1c receptor is a prominent serotonin receptor subtype in the central nervous system. *Proc. Natl. Acad. Sci. U.S.A.* **86**, 6793–6797 (1989).
85. H. Canton, R. B. Emeson, E. L. Barker, J. R. Backstrom, J. T. Lu, M. S. Chang, E. Sanders-Bush, Identification, molecular cloning, and distribution of a short variant of the 5-hydroxytryptamine2C receptor produced by alternative splicing. *Mol. Pharmacol.* **50**, 799–807 (1996).
86. M. Pasqualetti, M. Ori, M. Castagna, D. Marazziti, G. B. Cassano, I. Nardi, Distribution and cellular localization of the serotonin type 2C receptor messenger RNA in human brain. *Neuroscience* **92**, 601–611 (1999).
87. J. Lappalainen, L. Zhang, M. Dean, M. Oz, N. Ozaki, D.-h. Yu, M. Virkkunen, F. Weight, M. Linnoila, D. Goldman, Identification, expression, and pharmacology of a Cys23-Ser23 substitution in the human 5-HT_{2c} receptor gene (HTR2C). *Genomics* **27**, 274–279 (1995).
88. E. Xie, L. Zhu, L. Zhao, L.-S. Chang, The human serotonin 5-HT_{2C}receptor: Complete cDNA, genomic structure, and alternatively spliced variant. *Genomics* **35**, 551–561 (1996).
89. C. M. Burns, H. Chu, S. M. Rueter, L. K. Hutchinson, H. Canton, E. Sanders-Bush, R. B. Emeson, Regulation of serotonin-2C receptor G-protein coupling by RNA editing. *Nature* **387**, 303–308 (1997).
90. S. Maas, S. Patt, M. Schrey, A. Rich, Underediting of glutamate receptor GluR-B mRNA in malignant gliomas. *Proc. Natl. Acad. Sci. U.S.A.* **98**, 14687–14692 (2001).
91. B. L. Roth, M. W. Hamblin, R. D. Ciaranello, Developmental regulation of 5-HT_2 and 5-HT_{1c} mRNA and receptor levels. *Brain Res. Dev. Brain Res.* **58**, 51–58 (1991).
92. L. H. Tecott, L. M. Sun, S. F. Akana, A. M. Strack, D. H. Lowenstein, M. F. Dallman, D. Julius, Eating disorder and epilepsy in mice lacking 5-HT^{2c} serotonin receptors. *Nature* **374**, 542–546 (1995).
93. S. Kishore, S. Stamm, The snoRNA HBII-52 regulates alternative splicing of the serotonin receptor 2C. *Science* **311**, 230–232 (2006).
94. L. Oruc, G. R. Verheyen, I. Furac, M. Jakovljević, S. Ivezić, P. Raeymaekers, C. Van Broeckhoven, Association analysis of the 5-HT2C receptor and 5-HT transporter genes in bipolar disorder. *Am. J. Med. Genet.* **74**, 504–506 (1997).
95. B. Gutiérrez, B. Arias, S. Papiol, A. Rosa, L. Fañanás, Association study between novel promoter variants at the 5-HT2C receptor gene and human patients with bipolar affective disorder. *Neurosci. Lett.* **309**, 135–137 (2001).
96. R. H. Segman, U. Heresco-Levy, B. Finkel, R. Inbar, T. Neeman, M. Schlafman, A. Dorevitch, A. Yakir, A. Lerner, T. Goltser, A. Shelevoy, B. Lerer, Association between the serotonin 2C receptor gene and tardive dyskinesia in chronic schizophrenia: Additive contribution of 5-HT2Cser and DRD3gly alleles to susceptibility. *Psychopharmacology* **152**, 408–413 (2000).
97. C. Holmes, M. J. Arranz, J. F. Powell, D. A. Collier, S. Lovestone, 5-HT_{2A} and 5-HT_{2C} receptor polymorphisms and psychopathology in late onset Alzheimer's disease. *Hum. Mol. Genet.* **7**, 1507–1509 (1998).
98. I. Gurevich, H. Tamir, V. Arango, A. J. Dwork, J. J. Mann, C. Schmauss, Altered editing of serotonin 2C receptor pre-mRNA in the prefrontal cortex of depressed suicide victims. *Neuron* **34**, 349–356 (2002).
99. S. Dracheva, N. Patel, D. A. Woo, S. M. Marcus, L. J. Siever, V. Haroutunian, Increased serotonin 2C receptor mRNA editing: A possible risk factor for suicide. *Mol. Psychiatry* **13**, 1001–1010 (2008).
100. M. S. K. Sodhi, E. Sanders-Bush, Serotonin and brain development. *Int. Rev. Neurobiol.* **59**, 111–174 (2004).

Acknowledgments: We thank the Comparative Genomics Laboratory staff at the National Institute of Genetics for supporting genome sequencing. Some of the monkeys in this study were provided by the National BioResource Project "Japanese Monkeys" of the Ministry of Education, Culture, Sports, Science and Technology of Japan. **Funding:** This work was supported by a Grant-in-Aid for Japan Society for the Promotion of Science (JSPS) Fellows to K.Y. (21-4142) and Y.G. (24650234, 26640065); by a Grant-in-Aid for Scientific Research on Innovative Areas "Genome Science" to Y.G., A.T., and A.F. (221S0002); by the National Institutes of Natural Sciences program for cross-disciplinary study to Y.G.; by "Integrated research on neuropsychiatric disorders" carried out under the Strategic Research Program for Brain Sciences and the Brain Mapping by Integrated Neurotechnologies for Disease Studies (Brain/MINDS) to Y.G., I.K., and N.O. from the Japan Agency for Medical Research and Development; by Precursory Research for Embryonic Science and Technology to M.I.; by the Brain Sciences Project of the Center for Novel Science Initiatives, the National Institutes of Natural Sciences to Y.G. (BS241005) and M.I. (BS251001); and, in part, by JSPS KAKENHI to M.I. (15H04262). This work was supported by the Cooperative Research Program of the Primate Research Institute, Kyoto University. **Author contributions:** K.Y. and M.I. conceived the experiments. K.Y., N.S., A.I., and M.I. designed, performed, and analyzed the behavioral and neurophysiological experiments. Y.G., A.T., and A.F. designed, performed, and analyzed the exome sequencing experiments. I.K., H.I., and N.O. designed, performed, and analyzed the CNV experiments. The paper was written by K.Y., Y.G., I.K., N.O., and M.I. and was edited by the other authors. **Competing interests:** The authors declare that they have no competing interests. **Data and materials availability:** All data needed to evaluate the conclusions in the paper are present in the paper and/or the Supplementary Materials. Additional data related to this paper may be requested from the authors.

Submitted 15 March 2016
Accepted 17 August 2016
Published 21 September 2016
10.1126/sciadv.1600558

Citation: K. Yoshida, Y. Go, I. Kushima, A. Toyoda, A. Fujiyama, H. Imai, N. Saito, A. Iriki, N. Ozaki, M. Isoda, Single-neuron and genetic correlates of autistic behavior in macaque. *Sci. Adv.* **2**, e1600558 (2016).

ScienceAdvances
AAAS

Single-neuron and genetic correlates of autistic behavior in macaque

Kyoko Yoshida, Yasuhiro Go, Itaru Kushima, Atsushi Toyoda, Asao Fujiyama, Hiroo Imai, Nobuhito Saito, Atsushi Iriki, Norio Ozaki and Masaki Isoda (September 21, 2016)
Sci Adv 2016, 2:.
doi: 10.1126/sciadv.1600558